FOREX Publication
Open Access | Rapid and quality publishing

International Journal of
Electrical and Electronics Research (IJEER)
Research Article | Volume 12, Issue 1 | Pages 203-210 | e-ISSN: 2347-470X

Performance Evaluation and Dynamic Characteristics of a Self-Excited Induction Generator for Pico Hydro Power Plants

Krismadinata[1,2*] and Derry Fiandri[2]
[1]*Centre for Energy and Power Electronics Research Universitas Negeri Padang, Indonesia*
[2]*Department of Electrical Engineering Universitas Negeri Padang, Indonesia*

***Correspondence:** krisma@ft.unp.ac.id

ABSTRACT- The dynamic performance of an isolated three-phase squirrel cage self-excited induction generator (SEIG) in a Pico Hydro Power Plant (PHPP) is examined in this work. The investigation is carried out with the help of MATLAB/Simulink for mathematical modeling and simulation of the proposed system under various operational situations. The SEIG model, which was created using the steady-state equivalent circuit approach, included the electrical, magnetic, and mechanical components of the SEIG and PHPP. The dynamic behavior of the SEIG is explored under a variety of operating situations. The effects of load variations, speed fluctuations, and other disturbances on the voltage and frequency of the generator are examined. The experiment results were used to validate the simulation results. This research has implications for the design and optimization of PHPP using SEIGs.

Keywords: Pico hydro power plant; Self-excited induction generator; Dynamic performance.

ARTICLE INFORMATION
Author(s): Krismadinata and Derry Fiandri;
Received: 21/10/2023; **Accepted**: 30/01/2024; **Published**: 15/04/2024;
e-ISSN: 2347-470X;
Paper Id: IJEER 2110-17;
Citation: 10.37391/IJEER.120129
Webpage-link:
https://ijeer.forexjournal.co.in/archive/volume-12/ijeer-120129.html

Publisher's Note: FOREX Publication stays neutral with regard to Jurisdictional claims in Published maps and institutional affiliations.

1. INTRODUCTION

Hydroelectricity is the most dependable and cost-effective renewable energy source in remote mountainous areas [1]. Remote mountainous regions rely heavily on small hydroelectric plants to satisfy their energy demands. Mini (less than 1000 kW), micro (less than 100 kW), and Pico (less than 5 kW) hydro systems are categorized according to their power generation capacity [2], [3].

Due to its ease of use, low cost, and self-excitation ability, a squirrel cage rotor SEIG is an ideal generator for Pico hydro power systems [4]– [7]. The system is made simpler and less expensive [8]– [11]. Nevertheless, for the purpose to ensure the steady and dependable operation of the PHPP system, the dynamic behaviour of SEIGs needs to be thoroughly investigated.

A three-phase squirrel-cage SEIG with balanced capacitors in the stator winding will be simulated and tested in this paper. The basic model technique uses the stator and rotor *d-q* axis magnetic flux connections as the state space variable. In deriving the mathematical model, the main magnetic flux saturation may be separated magnetic flux leakage saturation. State space solution of MATLAB package program will examine dynamic performance. The dynamic performance of the machine will be examined for initial self-excitation process, sudden increases and decreases in load, rapid variation in excitation capacitor value while under load and three phase short circuit in the stator terminal. The simulation result and experiment test result consist of the voltage and current waveforms for each of the dynamic conditions.

2. STRUCTURE OF PHPP

Figure 1 shows a typical PHPP. Hydroelectric power plants convert the potential energy of water (represented by its mass) and the kinetic energy of water (represented by its flow) into mechanical energy that can be used to turn the rotor of an electric generator [12]– [18].

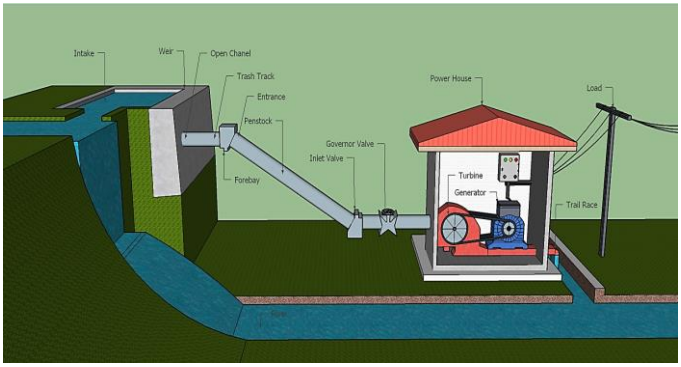

Figure 1. Composition of a typical PHPP

The mathematical expression for the amount of hydraulic energy existing in a given body of water, such as a river or stream, is.

$$P_{hyd} = \rho g Q H \quad (1)$$

In the given context, the variables P_{hyd}, ρ, g, Q, and H represent the following electrical engineering parameters: P_{hyd},

FOREX Publication
Open Access | Rapid and quality publishing
International Journal of Electrical and Electronics Research (IJEER)
Research Article | Volume 12, Issue 1 | Pages 203-210 | e-ISSN: 2347-470X

denotes the hydraulic power measured in Watts, ρ represents the water density of 1000 kg/m^3, g signifies the acceleration due to gravity of 9.8 m/s2, Q represents the effective flow rate measured in m3/s, and H denotes the effective head measured in meters.

Electricity production increases with flow or head. Due to system inefficiencies, electrical power will remain lower than hydraulic power. The system's final electrical power is calculated as:

$$P_F = \eta P_H \qquad (2)$$

The final electrical power (PF) is determined by the overall efficiency (η) of the system's components and the hydraulic power (PH or Phyd) in kilowatts (kW).

3. INDUCTION GENERATOR

Leading reactive power supplies excitation or magnetizing current to induction generators. AC sources attached to machines or capacitive reactance produce the most reactive power. The stator induction machine's real power, P, is negative when driven by an asynchronous motor faster than its synchronous speed from an alternating current voltage source. A magnetic field is created as reactive power, Q, passes from source to stator windings.

The magnetic field of the stator rotated at synchronous speed. This mode of operation is known as AC regenerative mode of induction machine. The prime mover's mechanical input power, P_m, is transformed into electricity and given to the source. Reactive power, however, continues to be used from the mains. *Figure 2* depicts the squirrel-cage setup with the excitation capacitor for the SEIG.

The mechanism of self-excitation involves the building up of magnetization flux form the interaction of induction machine with a bank of capacitor. Residual magnetism in the rotor causes the generator to act like a weak synchronous generator. When the shaft is rotated with the terminals open circuited, a small voltage is produced. If a large enough capacitance is connected to the terminals a current will be induced in the stator producing a flux that assists the residual lux this increased flux produces more voltage. The flux continues to build up to level that causes iron in the machine to saturate. The excitation will stabilize when the reactive power absorbed by the machine and the load equals the reactive power delivered by the capacitors. The saturation of the machine ensures that if the system self-excites there will be a point of stabilization.

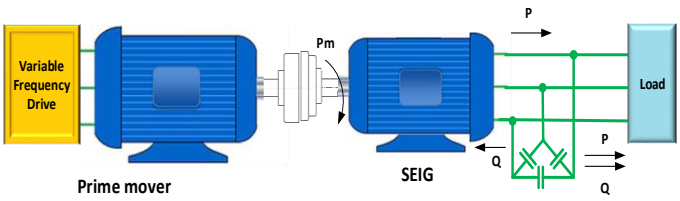

Figure 2. The Configuration of Squirrel-cage SEIG

4. MODELING OF SELF-EXCITED INDUCTION GENERATOR

The induction generator model may be used to investigate its many features. In order to simulate an induction generator, its parameters must be known. Traditionally, the parameters of the equivalent circuit model have been determined by approximation-free open-circuit (no load) and short-circuit (locked rotor) tests [19].

Typically, an orthogonal (*d-q*) coordinate system is used to depict the equations used to define the transitory performance of an induction machine. The mathematical model in terms of the d-q coordinate of a self-excited squirrel cage rotor induction generator with capacitor in the stator winding can be derived from the mathematical model of the induction machine presented in the references [20]– [23]. In this situation, the voltage and current equation are required to define the transient performance of a squirrel cage rotor SEIG.

The voltage equations of the stator and rotor windings in terms of the d-q axis are given by the following matrix equation.

$$\begin{bmatrix} v_{sq} \\ v_{sd} \\ 0 \\ 0 \end{bmatrix} = \begin{bmatrix} R_s & 0 & 0 & 0 \\ 0 & R_s & 0 & 0 \\ 0 & 0 & R'_r & 0 \\ 0 & 0 & 0 & R'_R \end{bmatrix} \begin{bmatrix} -i_{sq} \\ -i_{sd} \\ i_{rd} \\ i_{rd} \end{bmatrix} + \begin{bmatrix} 0 & \omega & 0 & 0 \\ -\omega & 0 & 0 & 0 \\ 0 & 0 & 0 & -(\omega - \omega_r) \\ 0 & 0 & -(\omega - \omega_r) & 0 \end{bmatrix} \begin{bmatrix} \lambda_{sq} \\ \lambda_{sd} \\ \lambda_{rd} \\ \lambda_{rd} \end{bmatrix} + \frac{d}{dt} \begin{bmatrix} \lambda_{sq} \\ \lambda_{sd} \\ \lambda_{rd} \\ \lambda_{rd} \end{bmatrix} \qquad (3)$$

Where ω the arbitrary reference frame frequency and ω_r is is the rotor frequency. Since the rotor windings are short circuited, v_{rd} and v_{rq} can be connected as zero.

For a magnetically linear system, the flux linkages equation of the stator and rotor winding sin term of the d-q axis may be expressed as:

$$\begin{bmatrix} \lambda_{sq} \\ \lambda_{sd} \\ \lambda'_{rq} \\ \lambda'_{rd} \end{bmatrix} = \begin{bmatrix} L_s & 0 & M & 0 \\ 0 & L_s & 0 & M \\ 0 & M & L'_r & 0 \\ M & 0 & 0 & L'_R \end{bmatrix} \begin{bmatrix} -i_{sq} \\ -i_{sd} \\ i'_{rq} \\ i'_{rd} \end{bmatrix} \qquad (4)$$

Where: $L_s = L_{ls}+M$, $L'_r = L'_{ir}+M$, $L'_{lr} = \left(\frac{N_s}{N_r}\right)^2 L_{rs}$, $M = \frac{3}{2} L_m$

Positive stator current is often thought to flow out the terminal when an induction machine is being used as a generator. Following this notation, the flow linkage equation becomes (5). The current equation of the stator in term of the *d-q* axis may be expressed as:

$$\begin{bmatrix} i_{sq} \\ i_{sd} \end{bmatrix} = \begin{bmatrix} i_{lq} \\ i_{ld} \end{bmatrix} + \begin{bmatrix} 0 & \omega \\ -\omega & 0 \end{bmatrix} \begin{bmatrix} Q_{sq} \\ Q_{sd} \end{bmatrix} + \frac{d}{dt} \begin{bmatrix} Q_{sq} \\ Q_{sd} \end{bmatrix} \qquad (5)$$

The electric charge on the stator capacitor in terms of the *d-q* axis is given by following equation.

FOREX Publication
Open Access | Rapid and quality publishing
International Journal of Electrical and Electronics Research (IJEER)
Research Article | Volume 12, Issue 1 | Pages 203-210 | e-ISSN: 2347-470X

$$\begin{bmatrix} Q_{sq} \\ Q_{sd} \end{bmatrix} = \begin{bmatrix} C & 0 \\ 0 & C \end{bmatrix} \begin{bmatrix} v_{sq} \\ v_{sd} \end{bmatrix} \quad (6)$$

Whereby, the mutual capacitor is neglected.

Equation (3)-(6) suggest the equivalent circuit of a wound-rotor SEIG with capacitor in the stator winding as shown in *figure 3*. The electromagnetic torque which is generated by the machine, is given by the following equation.

$$T_e = -\frac{3}{2} * \frac{P}{2} L_m \left(i_{qs} * i_{qr} - i_{ds} * i_{dr} \right) \quad (7)$$

The mechanical equation use in the computation was accordingly written as:

$$T_e = -J \frac{2}{P} \frac{dw_r}{dt} + T_i \quad (8)$$

Where the input torque of shaft and J is the inertia of the system.

In *equations (3)-(8)* all the parameters except the magnetizing inductance is assumed to be affected by saturation. The saturation curve was determined when the machine driven by a DC motor at synchronous speed and the slip ring open circuited.

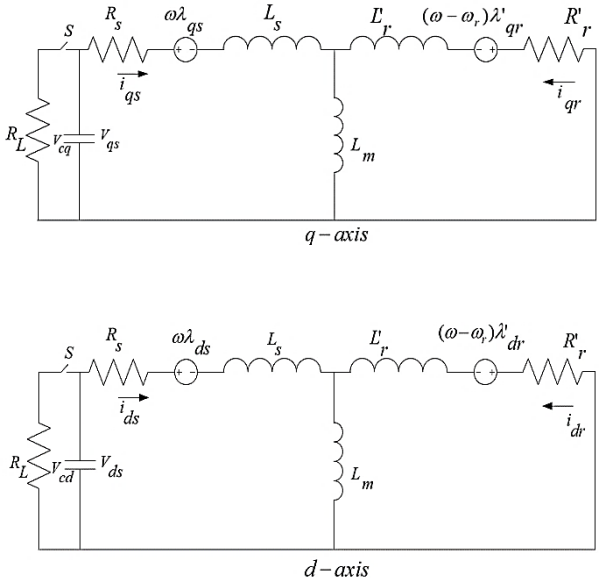

Figure 3. The equivalent circuit of a squirrel cage rotor SEIG with capacitor on the stator winding in terms of the d-q axis component

The curves were used to compute the saturated magnetizing current (L_m), and can be expressed as:

$$L_m = \frac{\lambda_m}{i_m} \quad (9)$$

The magnetizing current (i_m) can be expressed in the terms of the of the d-q axis as:

$$i_m^2 = (i_{ds} + i_{dr})^2 + \left(i_{qs} + i_{qr}\right)^2 \quad (10)$$

For the machine data in *table 1*, *figure 4* illustrates the magnetizing curve as a function of magnetizing current.

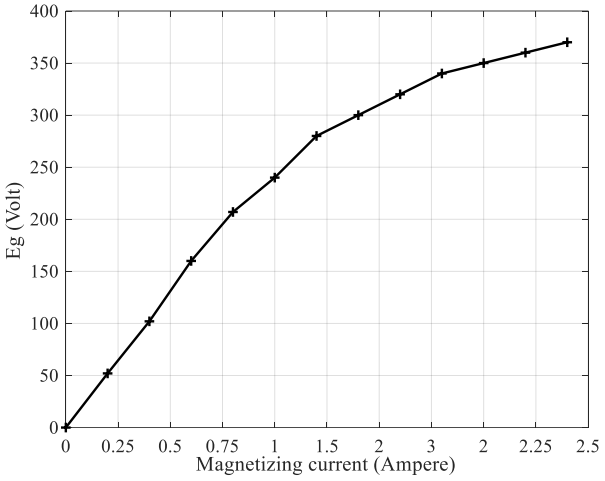

Figure 4. Magnetizing curve for the machine given in Table 1.

The analysis method adopted in saturated induction machines follows two main-stream approaches with respect to selection of state space variables. The first approach is modelling in terms of the stator and rotor d-q axis flux linkage component, while the second approach relies on stator and rotor d-q axis Currents as the state-space variable. The main feature of flux state-space model is that it is simpler than the current state-space model is used. The flux linkage *equation (4)* can be written as:

$$\begin{bmatrix} i_{sq} \\ i_{sd} \\ i'_{rq} \\ i'_{rd} \end{bmatrix} = \frac{1}{D} \begin{bmatrix} L'_r & 0 & -M & 0 \\ 0 & L'_r & 0 & -M \\ -M & 0 & L_s & 0 \\ 0 & -M & 0 & L_s \end{bmatrix} \begin{bmatrix} \lambda_{sq} \\ \lambda_{sd} \\ \lambda'_{rq} \\ \lambda'_{rd} \end{bmatrix} \quad (11)$$

Where $D = L_s.L'_r - M^2$, Substituting *equation (11)* to *equation (3)* and rearrangement of *equation (3)* will give the derivatives of the flux linkage equation as:

$$\begin{aligned} \frac{d\lambda_{sq}}{dt} &= -\frac{R_s L'_r}{D}\lambda_{sq} - \omega\lambda_{sd} + \frac{R_s M}{D}\lambda_{rq} + v_{sq} \\ \frac{d\lambda_{sd}}{dt} &= -\frac{R_s L'_r}{D}\lambda_{sd} + \omega\lambda_{sq} + \frac{R_s M}{D}\lambda_{rd} + v_{sd} \\ \frac{d\lambda'_{rq}}{dt} &= -\frac{R'_r M}{D}\lambda_{sq} - (\omega - \omega_r)\lambda_{rd} - \frac{R'_r L_s}{D}\lambda_{rq} \\ \frac{d\lambda'_{rd}}{dt} &= -\frac{R'_r M}{D}\lambda_{sd} + (\omega - \omega_r)\lambda_{rq} - \frac{R'_r L_s}{D}\lambda_{rd} \end{aligned} \quad (12)$$

Equation (10) can be expressed in state space terms as,

$$[\dot{\lambda}] = [A][\lambda] + [B][V] \quad (13)$$

Where [A] and [B] are the coefficient matrix.

$$A = \begin{bmatrix} \frac{-r_s L'_r}{D} & -\omega & \frac{r_s M}{D} & 0 \\ \omega & \frac{-r_s L'_r}{D} & 0 & \frac{r_s - M}{D} \\ \frac{r'_r M}{D} & 0 & \frac{-r'_r L_s}{D} & -(\omega - \omega_r) \\ 0 & \frac{r'_r M}{D} & (\omega - \omega_r) & \frac{-r'_r L_s}{D} \end{bmatrix}$$

FOREX Publication
Open Access | Rapid and quality publishing
International Journal of Electrical and Electronics Research (IJEER)
Research Article | Volume 12, Issue 1 | Pages 203-210 | e-ISSN: 2347-470X

$$B = \begin{bmatrix} 1 & 0 & 0 & 0 \\ 0 & 1 & 0 & 0 \\ 0 & 0 & 1 & 0 \\ 0 & 0 & 0 & 1 \end{bmatrix}$$

Equation (12) or (13) represents the transient performance of a squirrel cage rotor SEIG. During the initial self-excited process, the load RL is infinite, while during the three- phase short-circuit the stator voltage is to zero. The initial condition of the equation is used as the residual voltage across the stator terminal.

5. RESULTS AND DISCUSSION

Simulations with SIMULINK/MATLAB software determine the dynamic performance of a squirrel cage rotor SEIG with a capacitor in the stator winding. *Table 1* lists this investigation's SEIG induction machine specifications. SEIG is excited to 220V no-load voltage using a 20-µF per phase shunt excitation capacitor bank in delta connection.

Table 1. The parameter machine for SEIG

3 HP three phase squirrel cage rotor Induction Machine Parameters Value	Value
Rated Current (Is)	8.7/5.0 A
Rated Voltage (Vs)	380 /220 V
Stator Resistance (Rs)	2.9 Ω
Rotor Resistance (Rr)	8.28 Ω
Rotor Leakage Inductance (Llr)	26.456 mH
Stator Leakage Inductance (Lls)	26.456 mH
Magnetizing Inductance (Lm)	167 mH
Frequency (f)	50.0 Hz
Number of poles (N)	4
Rotation	1430 rpm
Connection	Δ/Y

Figure 5. Experiment setup for SEIG for various operating conditions

The investigation of the dynamic performance of a squirrel cage rotor three-phase SEIG is conducted by means of modelling, simulation, and experimentation under the specified operational Conditions:

- No-load voltage rise in an SEIG;
- Starting transients of the SEIG with various speed of prime mover at no-load;
- Transients of the SEIG with various excitation capacitors at no-load;
- Transients of the SEIG with various load;
- Transients of the SEIG with over load;
- Transients of the SEIG with various excitation capacitors at loaded.

Figure 5 shows the experimental setup. It is composed by induction machines. An electromechanical component associated with an induction motor with variable speed drives is used as prime mover and the one is employed to SEIG. Variable speed drive is used as a regulator of the rotor rotation rate.

5.1. No-load voltage rise in a SEIG

The process of generating the voltage at no-load that appears in the induction generator is done by rotating the induction generator rotor. *Figure 6* shows the magnetic remanence process that generates induced voltage on the stator side. The left side figure is simulation result and the right-side figure is experimenting result. This induced voltage is applied to the capacitor to produce a current that induces a voltage in the rotor coil. In the rotor coil, an induced *emf* will arise which is getting bigger so that it induces a voltage in the stator coil.

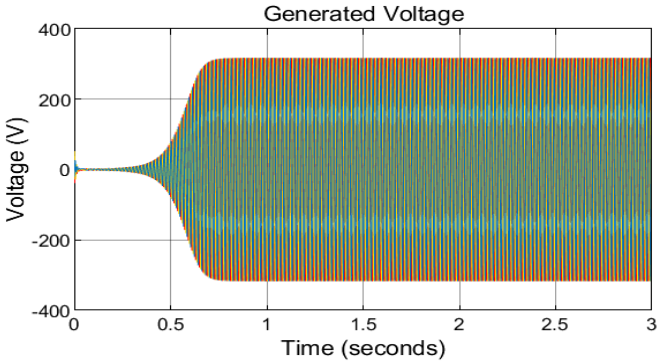

(a) Simulation

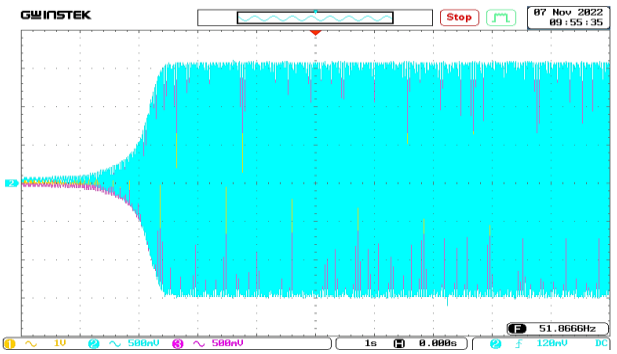

(b) Experiment

Figure 6. The voltage generation process

At this early stage, the field fluctuation is getting bigger, because the capacitor is always charging and discharging along

FOREX Publication
Open Access | Rapid and quality publishing
International Journal of Electrical and Electronics Research (IJEER)
Research Article | Volume 12, Issue 1 | Pages 203-210 | e-ISSN: 2347-470X

with sinusoidal voltage fluctuations in the stator and rotor. The generation of induced voltage in the stator coil will be greater so that the nominal voltage will be achieved. Once the nominal voltage is reached, the induction generator is ready to supply power to the load.

5.2. Transients of the SEIG with Various Speed of Prime Mover at No-Load

In a SEIG, the rotor speed affects the amount of voltage produced by the generator. *Figure 7* shows that when the rotor speed is increased, there is an increase in the voltage generated on the stator side. Meanwhile, *figure 8* shows the transient process when the voltage generated on the stator decreases when the rotor speed decreases.

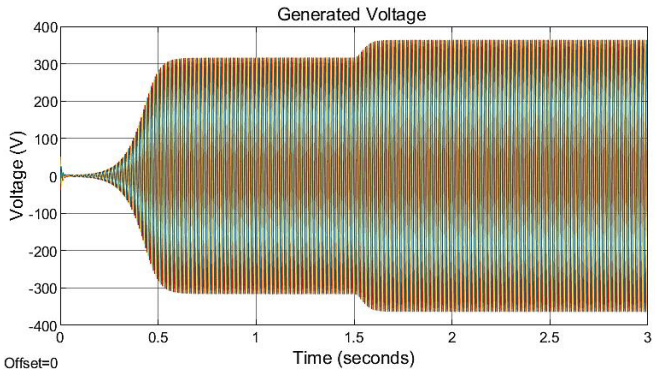

(a) Simulation

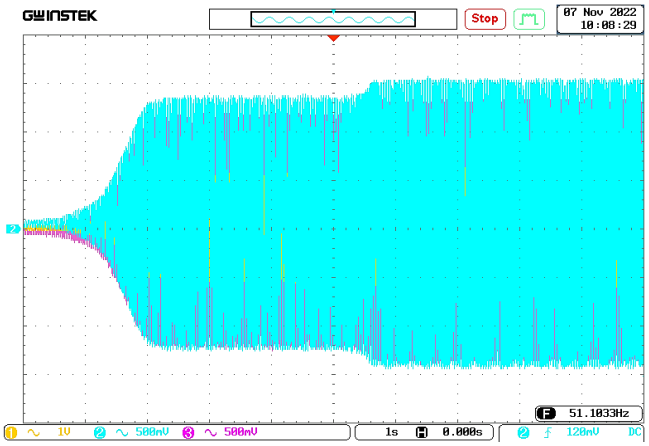

(b) Experiment

Figure 7. Speed increment at no load

Reduced rotor speed will cause a decrease in the frequency of the generated voltage. A decrease in voltage at the generator can affect the performance of the electrical system that uses the generator as a power source. Therefore, the rotor speed must be controlled and maintained at the right level so that the voltage produced remains stable and in accordance with the needs.

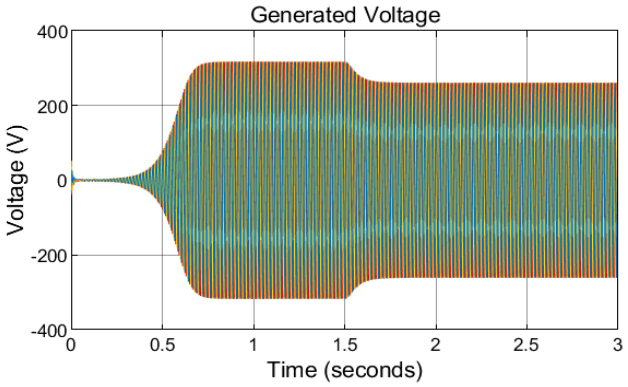

(a) Simulation

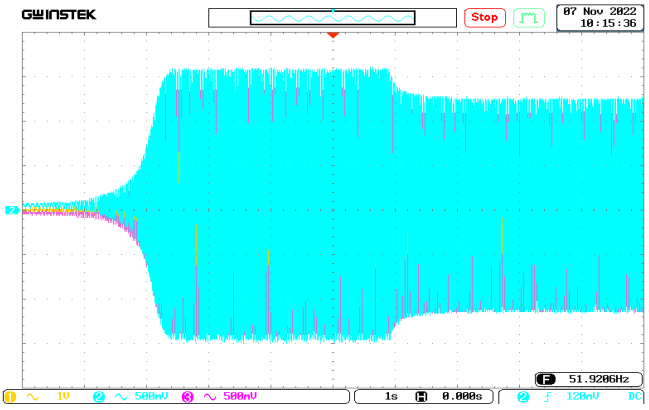

(b) Experiment

Figure 8. Capacitance value reduction at no Load

5.3. Transients of the SEIG with various excitation capacitors at No-Load

Excitation capacitors are used to meet reactive power needs in generating and maintaining a magnetic field when generating voltage. Increasing the value of the excitation capacitor will accelerate the generation of current and voltage and then strengthen the output signal. *Figure 9* shows the increase in voltage generated when the excitation capacitance is increased under these conditions the generator is in no load condition.

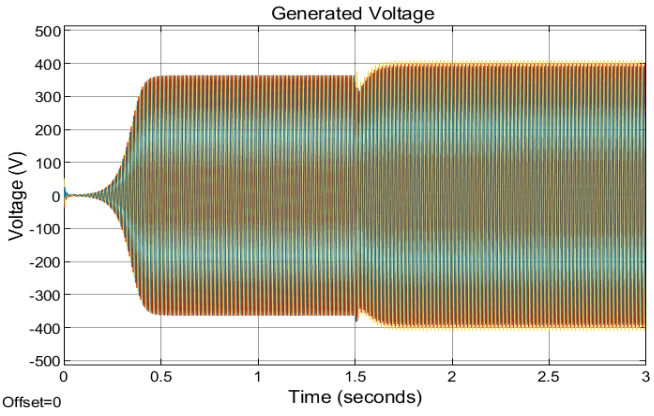

(a) Simulation

FOREX Publication
Open Access | Rapid and quality publishing
International Journal of Electrical and Electronics Research (IJEER)
Research Article | Volume 12, Issue 1 | Pages 203-210 | e-ISSN: 2347-470X

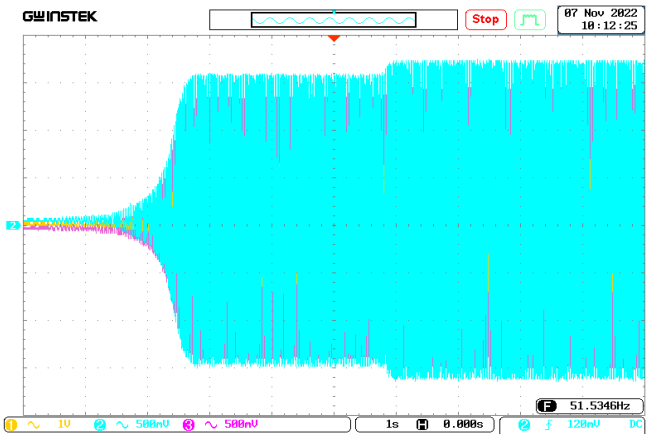

(b) Experiment

Figure 9. Increasing excitation capacitor value at no load

Figure 10 shows the decrease in voltage generated at no load condition SEIG when the excitation capacitance value is minimized. The voltage of SEIG increases and frequency decreases when the excitation capacitor value is increased due to changes in the RLC resonant circuit. The excitation capacitor forms a resonant circuit with the rotor induction and generator load. Increasing the value of the excitation capacitor will accelerate the resonant frequency of the circuit, thereby reducing the output frequency of the generator. However, an increase in the resonant frequency will also increase the amplitude of the resonant voltage, thereby increasing the output voltage of the generator.

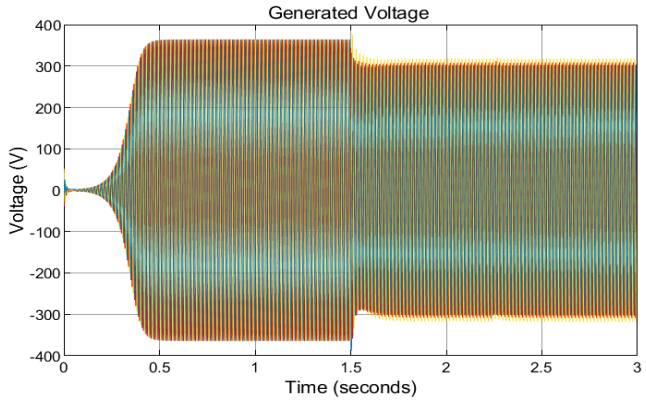

(a) Simulation

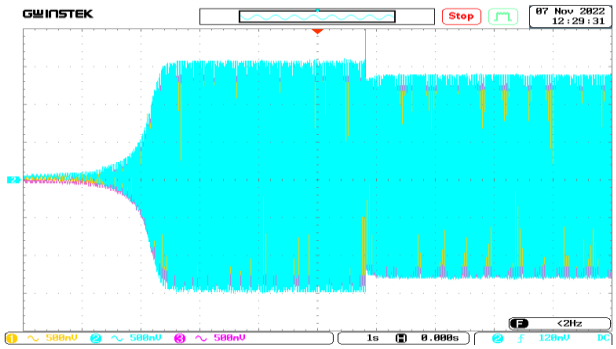

(b) Experiment

Figure 10. Capacitance value reduction at no Load

The reduction of the excitation capacitor value will minimize the resonant frequency of the circuit, thereby increasing the output frequency of the generator. However, reducing the resonant frequency will also reduce the amplitude of the resonant voltage, thereby reducing the output voltage of the generator.

5.4. Transients of the SEIG with various load

A number of incandescent lamps installed per-phase are employed as loads for the voltage output of the induction generator. The output voltage will decrease as the load increases. The dynamic condition of the SEIG can be seen in *figure 11*, which was created when the load was increased. The change in load is shown by the increase in load current and the decrease in voltage generated.

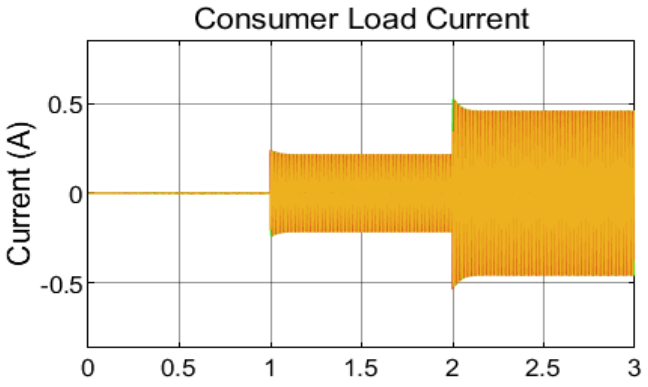

(a) Simulation

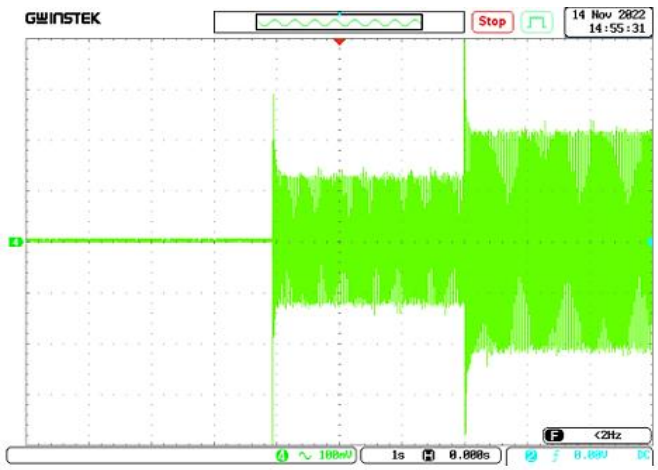

(b) Experiment

Figure 11. Increased Load

5.5. Transients of the SEIG with over load

In *figure 12*, it shows the induction generator is overloaded. The output voltage of the induction generator drops and even disappears when the generator load exceeds its limit. This is due to the inability of the induction generator to maintain the flux it generates.

FOREX Publication
Open Access | Rapid and quality publishing
International Journal of Electrical and Electronics Research (IJEER)
Research Article | Volume 12, Issue 1 | Pages 203-210 | e-ISSN: 2347-470X

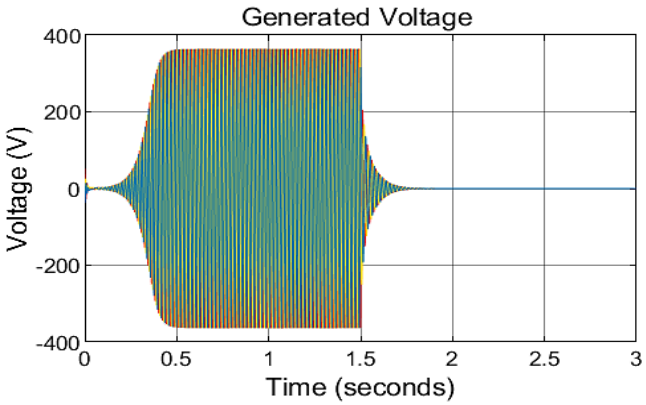

(a) Simulation

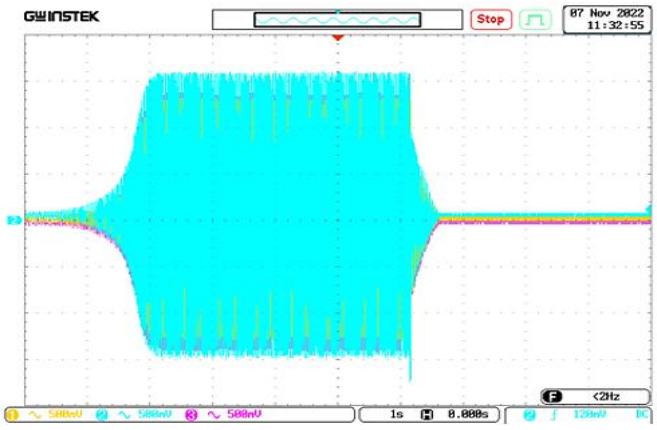

(b) Experiment

Figure 12. The voltage loss under overload

5.6. Transients of the SEIG with various excitation capacitors at load

If the excitation capacitor value is increased when the generator is loaded, the output voltage and load current will increase, and the load power factor will improve. If the excitation capacitor value is increased when the generator is resiliently loaded, the load current will increase. This is due to the increase in output voltage leading to an increase in load current. *(See figure 13).*

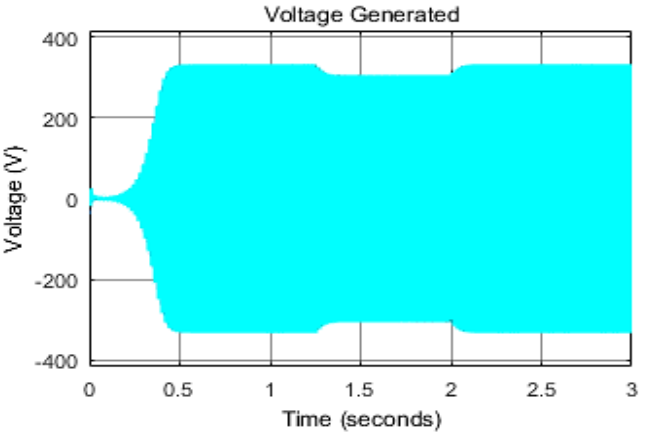

(a) Simulation

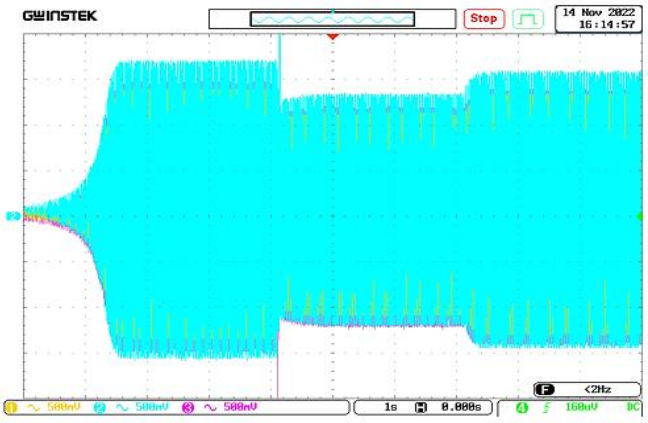

(b) Experiment

Figure 13. Increase in Excitation Capacitor Value under Load

Conversely, if the excitation capacitor value is reduced when the generator is loaded, the output voltage and load current will decrease. If the excitation capacitor value is reduced when the generator is resiliently loaded, the load current will decrease. This is due to the decrease in output voltage leading to a decrease in load current.

6. CONCLUSIONS

Analysis of a SEIG pico hydro power plant was done. Remainder magnetism in the stator core self-excited the generator. Using a mathematical model that accounted for load and rotor speed effects on output voltage and frequency, the generator worked effectively under varying loads. This illustrates small-scale hydropower from self-excited induction generators.

Pico hydro power plant self-excited induction generator dynamics and performance are analyzed in this study. Results can improve small-scale renewable energy plant efficiency and reliability. The squirrel-cage SEIG protection and control design challenges can be identified using transient simulation and experiment data. According to simulation and experiment data, squirrel-cage rotor SEIG protection is not needed during stator terminal short circuit events.

This study provides a better understanding of Pico hydro power plant SEIG. With its insights into generator design and operation, it helps achieve sustainable and eco-friendly power generation.

Acknowledgments: The PDPTLN Scheme at LPPM Universities Negeri Padang and the Ministry of Education, Culture, Research, and Technology of the Republic of Indonesia generously offered financial support to the authors. The project 1014/UN35.13/LT/2021.

REFERENCES

[1] A. N. Bachtiar, A. F. Pohan, Santosa, I. Berd, and U. G. S. Dinata, "Performance on compressor as turbine (CAT) piko hydro scale," *International Journal of Renewable Energy Research*, vol. 9, no. 4, 2019, doi: 10.20508/ijrer.v9i4.9331.g7830.

International Journal of Electrical and Electronics Research (IJEER)
Research Article | Volume 12, Issue 1 | Pages 203-210 | e-ISSN: 2347-470X

[2] M. Shah and S. Somkun, "Efficiency Evaluation of Three Phase and Single Phase C2C Self-Excited Induction Generator for Micro Hydro Power Application," in *Energy Procedia*, 2017. doi: 10.1016/j.egypro.2017.10.149.

[3] S. J. Williamson, B. H. Stark, and J. D. Booker, "Low head pico hydro turbine selection using a multi-criteria analysis," *Renew Energy*, vol. 61, 2014, doi: 10.1016/j.renene.2012.06.020.

[4] R. C. Bansal, "Three-phase self-excited induction generators: An overview," *IEEE Transactions on Energy Conversion*, vol. 20, no. 2. 2005. doi: 10.1109/TEC.2004.842395.

[5] D. Seyoum, C. Grantham, and M. F. Rahman, "The dynamic characteristics of an isolated self-excited induction generator driven by a wind turbine," *Conference Record-IAS Annual Meeting (IEEE Industry Applications Society)*, vol. 2, 2002, doi: 10.1109/IAS.2002.1042641.

[6] M. K. Rajak, J. Samanta, and R. Pudur, "A hardware-based novel approach for parallel operation of two differently rated SEIGs," *Results in Engineering*, vol. 17, 2023, doi: 10.1016/j.rineng.2022.100825.

[7] H. Faraji, N. Yavari Beigvand, and R. Hemmati, "Multi-objective and resilient control on hybrid wind farms under healthy/faulty and off-grid/grid-tied states," *Electric Power Systems Research*, vol. 215, 2023, doi: 10.1016/j.epsr.2022.109004.

[8] A. Serrano-Fontova and R. Bakhshi-Jafarabadi, "A new hybrid islanding detection method for mini hydro-based microgrids," *International Journal of Electrical Power and Energy Systems*, vol. 143, 2022, doi: 10.1016/j.ijepes.2022.108437.

[9] V. B. M. Krishna, V. Sandeep, S. S. Murthy, and K. Yadlapati, "Experimental investigation on performance comparison of self-excited induction generator and permanent magnet synchronous generator for small scale renewable energy applications," *Renew Energy*, vol. 195, 2022, doi: 10.1016/j.renene.2022.06.051.

[10] M. F. Khan, M. R. Khan, and A. Iqbal, "Effects of induction machine parameters on its performance as a standalone self-excited induction generator," *Energy Reports*, vol. 8, 2022, doi: 10.1016/j.egyr.2022.01.023.

[11] S. Al-Senaidi, A. Alolah, and M. Alkanhal, "Parallel operation of three-phase self-excited induction generators with different numbers of poles," *Engineering Science and Technology, an International Journal*, vol. 25, 2022, doi: 10.1016/j.jestch.2021.04.007.

[12] S. Praptodiyono, H. Maghfiroh, M. Nizam, C. Hermanu, and A. Wibowo, "Design and Prototyping of Electronic Load Controller for Pico Hydropower System," *Jurnal Ilmiah Teknik Elektro Komputer dan Informatika*, vol. 7, no. 3, 2021, doi: 10.26555/jiteki.v7i3.22271.

[13] W. Uddin *et al.*, "Current and future prospects of small hydro power in Pakistan: A survey," *Energy Strategy Reviews*, vol. 24. 2019. doi: 10.1016/j.esr.2019.03.002.

[14] L. N. Mbele, K. Kusakana, and S. P. Koko, "Simulations and experimental validation of Pico conduit pressure hydropower systems with battery storage," *J Energy Storage*, vol. 26, 2019, doi: 10.1016/j.est.2019.100976.

[15] N. F. Yah, A. N. Oumer, and M. S. Idris, "Small scale hydro-power as a source of renewable energy in Malaysia: A review," *Renewable and Sustainable Energy Reviews*, vol. 72. 2017. doi: 10.1016/j.rser.2017.01.068.

[16] V. K. Singh and S. K. Singal, "Operation of hydro power plants-a review," *Renewable and Sustainable Energy Reviews*, vol. 69. 2017. doi: 10.1016/j.rser.2016.11.169.

[17] H. S. Sachdev, A. K. Akella, and N. Kumar, "Analysis and evaluation of small hydropower plants: A bibliographical survey," *Renewable and Sustainable Energy Reviews*, vol. 51. 2015. doi: 10.1016/j.rser.2015.06.065.

[18] M. K. Mishra, N. Khare, and A. B. Agrawal, "Small hydro power in India: Current status and future perspectives," *Renewable and Sustainable Energy Reviews*, vol. 51. 2015. doi: 10.1016/j.rser.2015.05.075.

[19] O. Ejiofor, C. Nwosu, and M. Agu, *Dynamic Modeling of Self-Excited Induction Generator for Enhanced Power Generation*. 2013.

[20] Y. Chaturvedi, S. Kumar, and V. Gupta, "Capacitance Requirement for Rated Current and Rated Voltage Operation of SEIG Using Whale Optimization Algorithm," in *Procedia Computer Science*, 2020. doi: 10.1016/j.procs.2020.03.315.

[21] S. K. Saha and K. S. Sandhu, "Optimization Techniques for the Analysis of Self-excited Induction Generator," in *Procedia Computer Science*, 2018. doi: 10.1016/j.procs.2017.12.053.

[22] Y. J. Wang and S. Y. Liu, "Simulation of a Self-excited Three-phase Induction Generator Using the EMTP/ATP," in *Energy Procedia*, 2017. doi: 10.1016/j.egypro.2017.10.087.

[23] G. K. Singh, "Self-Excited Induction Generator for Renewable Applications," in *Encyclopedia of Sustainable Technologies*, M. A. Abraham, Ed., Oxford: Elsevier, 2017, pp. 239–256. doi: https://doi.org/10.1016/B978-0-12-409548-9.10132-0.

© 2024 by the Krismadinata and Derry Fiandri. Submitted for possible open access publication under the terms and conditions of the Creative Commons Attribution (CC BY) license (http://creativecommons.org/licenses/by/4.0/).